Electronic supplementary information

High-Performance Self-Powered $CsPbBr_3$ Perovskite Photodetector Enabled by Self-Assembled Monolayer Interface Engineering

Yu Liu[1], Li Chen[1,*], Shaohong Li[1], Zejiang Gao[1], Yuping Pang[1], Bingsuo Zou[2,*]

1 School of Physical Science and Technology, State Key Laboratory of Featured Metal Materials and Life-cycle Safety for Composite Structures, Guangxi University, Nanning 530004, China.

2 School of Resources, Environments and Materials, Guangxi University, Nanning 530004, China

Corresponding Authors

*E-mail: chenli@gxu.edu.cn (L. Chen), zoubs@gxu.edu.cn (B. Zou)

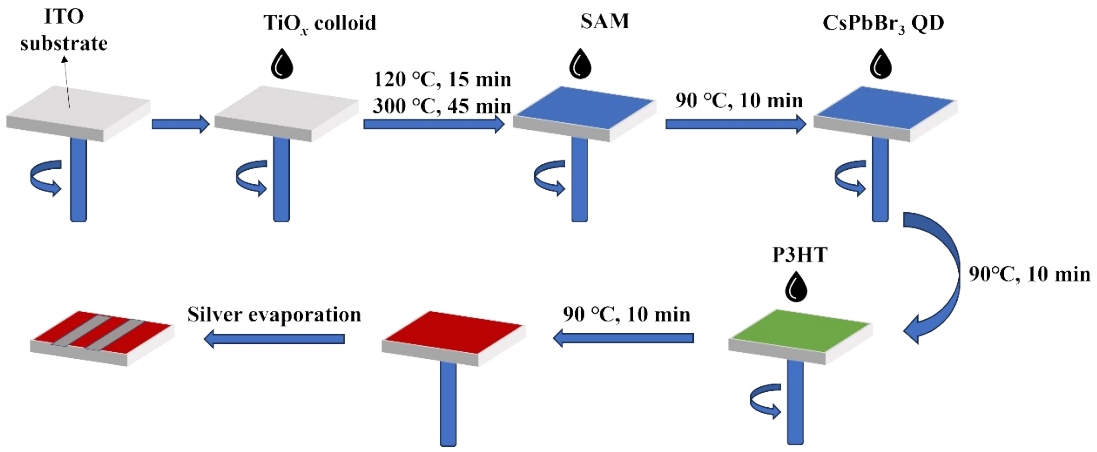

Figure S1. Schematic diagram of the fabrication of a self-powered photodetector.

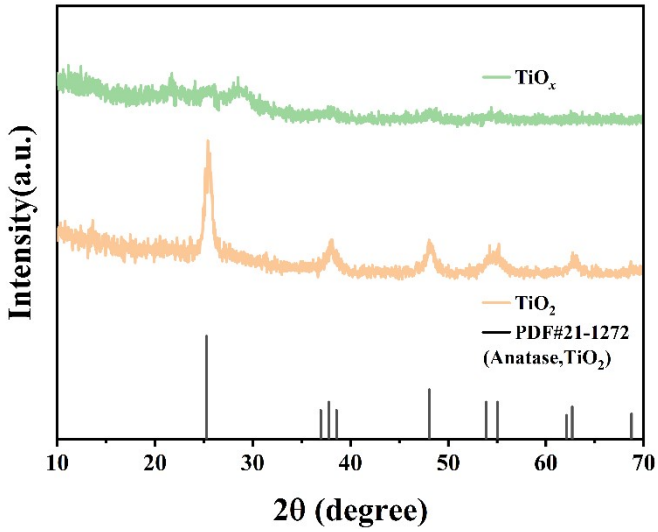

Figure S2. XRD analysis of the TiO_2 film annealed at high temperature (500 °C) versus the TiO_x film annealed at low temperature (300 °C). The TiO_2 film is identified as the anatase phase, whereas the low-temperature TiO_x film is evidently amorphous.

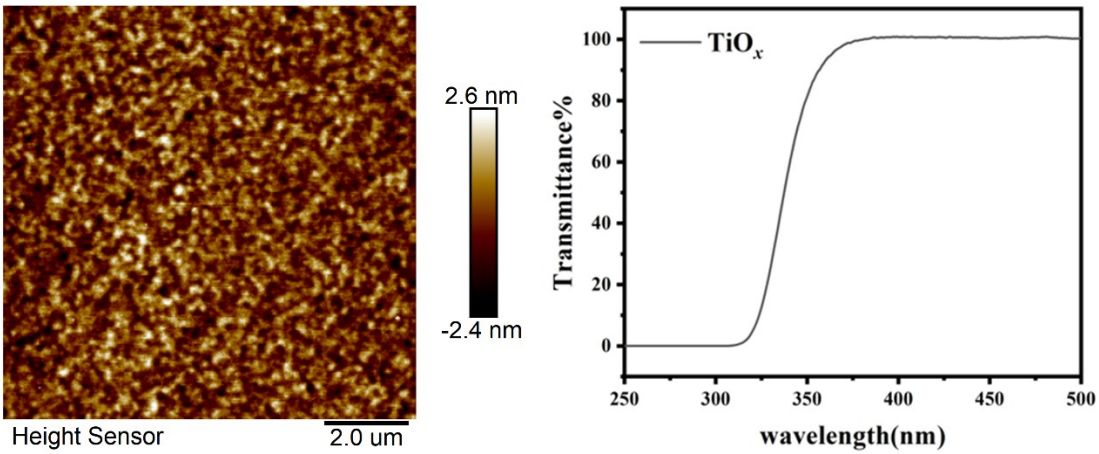

Figure S3. The surface morphology of TiO_x was measured by AFM (left) and its transmission spectrum (right).

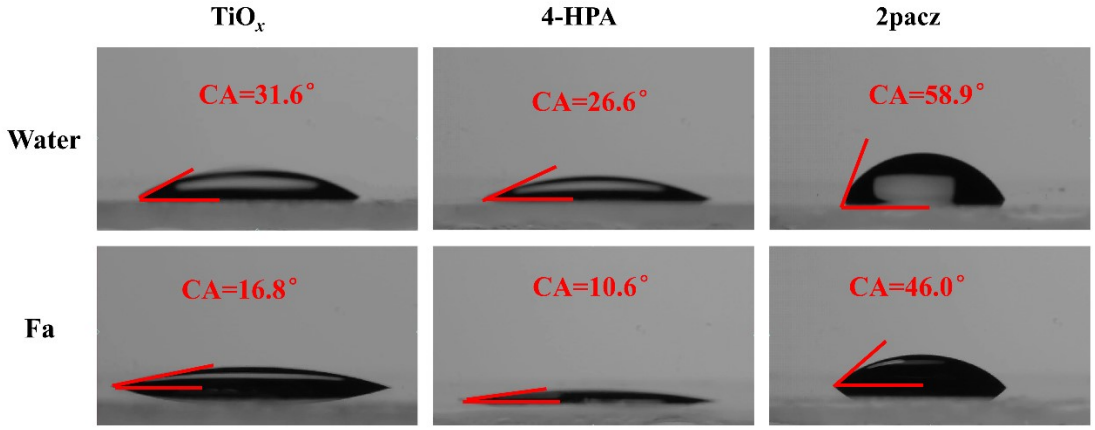

Figure S4. Digital photographs showing the corresponding contact angles of water droplets and formamide droplets on the original surface or SAM-modified surface.

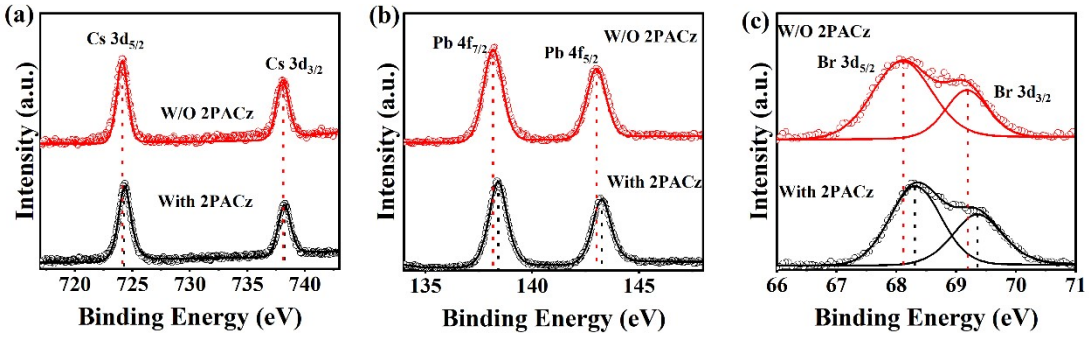

Figure S5. High-resolution XPS spectra of (a) Cs 3d, (b) Pb 4f, and (c) Br 3d for unmodified and 2PACz-modified $CsPbBr_3$ samples.

The Cs $3d_{3/2}$ and Cs $3d_{5/2}$ peaks shift from 738.05 and 724.11 eV to 738.20 and 724.26 eV. Similarly, the Pb $4f_{5/2}$ and Pb $4f_{7/2}$ peaks shift from 143.00 eV and 138.16 eV to 143.23 eV and 138.39 eV, while the Br $3d_{3/2}$ and Br $3d_{5/2}$ peaks shift from 69.18 eV and 68.10 eV to 69.39 eV and 68.31 eV.

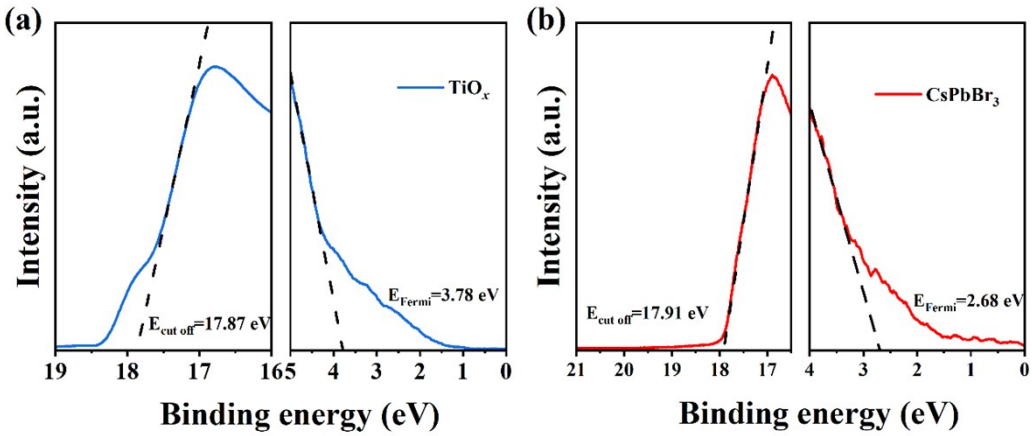

Figure S6. UPS spectrums of (a) TiO_x and (b) $CsPbBr_3$.

The energy level position can be calculated using the following formula:

$$21.22 - VBM = E_{cut\ off} - E_{Fermi} \quad (1)$$

$$CBM = VBM + E_g \quad (2)$$

Where E_{cutoff}, CBM, VBM, E_{Fermi}, and E_g represent the cutoff energy, conduction band maximum, valence band maximum, Fermi level, and bandgap, respectively.

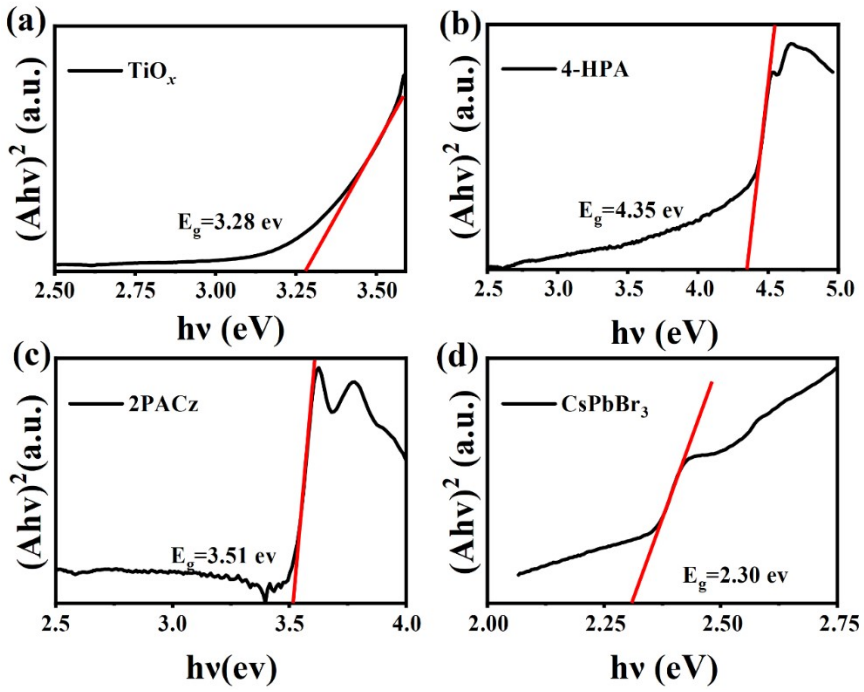

Figure S7. Tauc plot determines the corresponding E_g values of the films: (a) 3.28 eV, (b) 4.35 eV, (c) 3.51 eV, and (d) 2.30 eV.

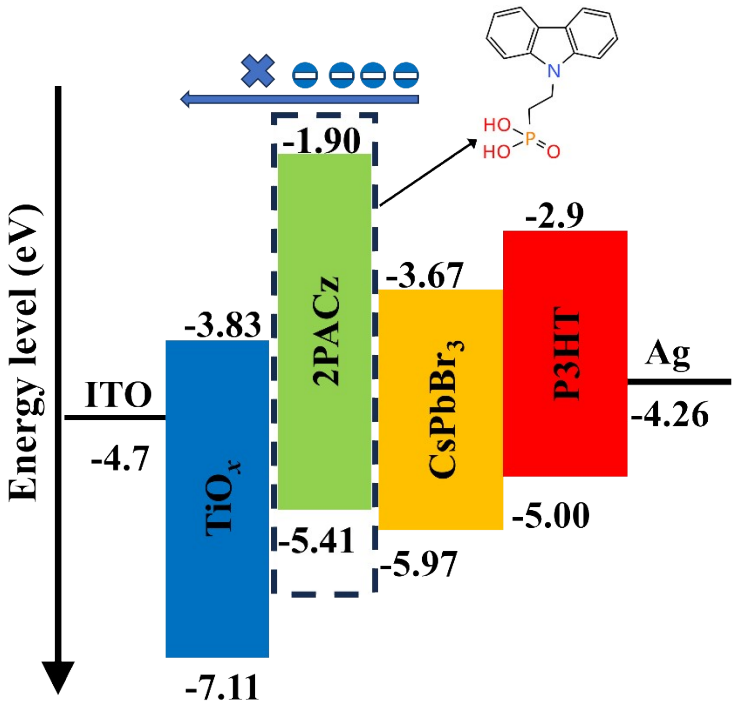

Figure S8. The energy band diagram of the 2PACz modified device.

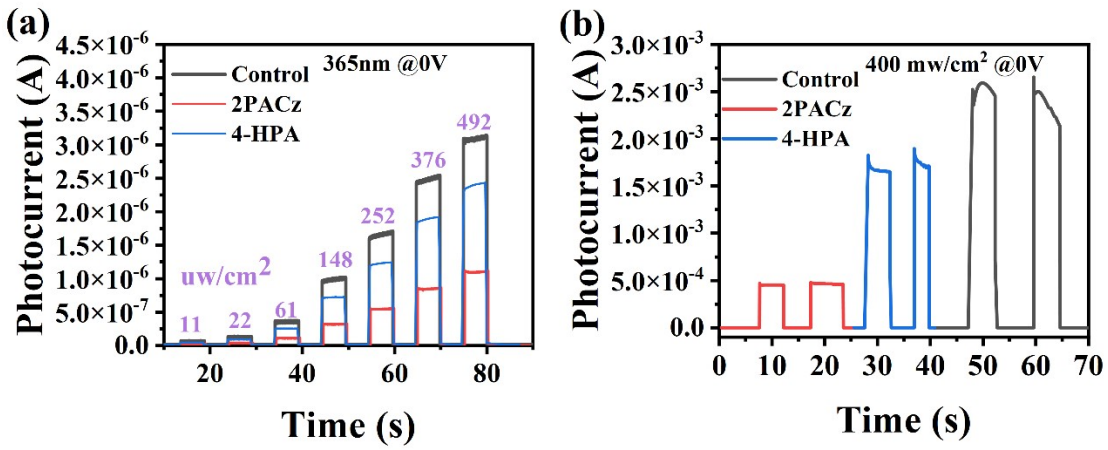

Figure S9. Comparison of device photocurrent response under (a) low light intensity and (b) high light intensity.

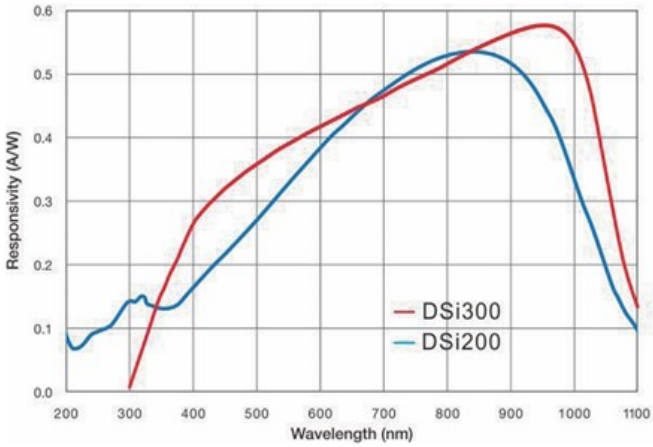

Figure S10. Spectral responsivity curves of two types of commercial silicon photodetectors.[45]

The commercial UV-enhanced silicon photodiode DSi200 exhibits a responsivity of approximately 130 mA/W and a specific detectivity of approximately 2.2 × 10^{12} Jones when operating at 365 nm under a 10 V bias.

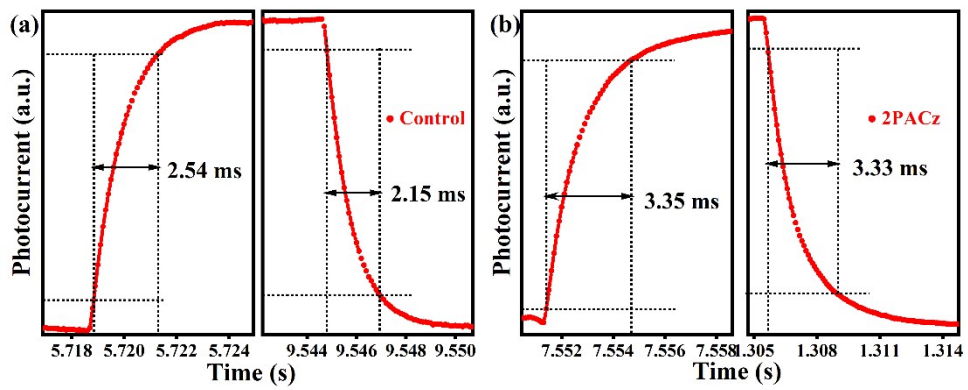

Figure S11. Response time of the original and 2PACz-modified devices.

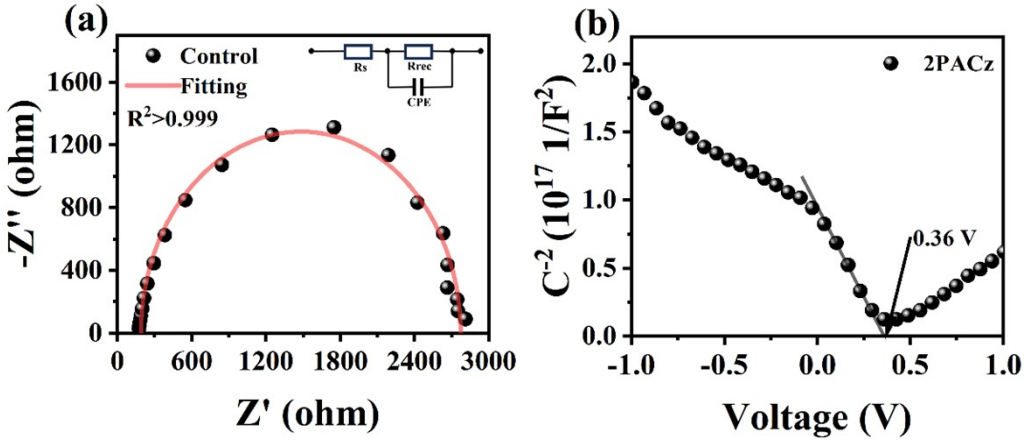

Figure S12. EIS of the 2PACz-modified device and Mott-Schottky measurement of the original device.

Table S1. Parameters in the bi-exponential fitting equation of the TRPL decay profiles.

	A_1 (%)	t_1 (ns)	A_2 (%)	t_2 (ns)	τ_{avg} (ns)
Control	69	2.15	31	12.51	9.62
2PACz	68	2.36	32	13.71	10.69
4-HPA	68	3.38	32	16.80	12.76

Table S2. Performance of the original, 2PACz, and 4-HPA modified photodetectors.

	I_{ph} (A)	I_{dark} (A)	*LDR* (dB)	t_r (ms)	t_f (ms)	*R* (mA/W)	D^* (Jones)	*K*	EQE
Control	4.56×10^{-4}	9.66×10^{-9}	108.2	2.54	2.15	139.0	5.00×10^{11}	4.72×10^{-4}	47.2%
2PACz	1.12×10^{-4}	1.50×10^{-9}	110.4	3.35	3.33	34.1	3.12×10^{11}	7.47×10^{-4}	11.6%
4-HPA	3.59×10^{-4}	2.18×10^{-10}	137.7	2.10	2.37	109.5	2.62×10^{12}	1.65×10^{-6}	37.2%

Table S3. Performance of the DSi200 and 4-HPA modified photodetectors.

	S (cm^2)	Bias (V)	*R* (mA/W)	D^* (Jones)
DSi200	1	10	130	2.20×10^{12}
4-HPA	0.04	0	115	2.74×10^{12}

References

45. Zolix Instruments Co., Ltd., Silicon Photodiode Technical Datasheet. URL: https://zolix.com.cn/filespath/files/guangpu/DSi200.pdf (accessed 5 June 2024).